Proceedings of the 19th International Symposium on the Packaging and Transportation of Radioactive Materials
PATRAM 2019
August 4-9, 2019, New Orleans, LA, USA

Modeling and Analysis of Used Nuclear Fuel during Normal Conditions of Rail Transportation

Nicholas Klymyshyn
Pacific Northwest National Laboratory (PNNL)

Pavlo Ivanusa	**Kevin Kadooka**	**Casey Spitz**	**Philip Jensen**
PNNL	PNNL	PNNL	PNNL

ABSTRACT
In 2017, the United States Department of Energy collaborated with Spanish and Korean organizations to perform a multimodal transportation test (MMTT) to measure shock and vibration loads imparted to used nuclear fuel (UNF) assemblies. This test used real fuel assembly components containing surrogate fuel mass to approximate the response characteristics of irradiated used nuclear fuel. Pacific Northwest National Laboratory (PNNL) was part of the test team and performed modeling and analysis using the test data to validate numerical models and analysis methods to predict the dynamic response of the cask and conveyance system, including the structural-dynamic response of fuel assemblies and fuel cladding. The analysis chain begins with a railcar dynamics model using the NUCARS railcar dynamics software to estimate the dynamic response of the conveyance system to the speed and a specified track geometry. The NUCARS model calculates the response of the conveyance system up to the cask. The cask motion is then used as an input to structural-dynamic models of the fuel assembly or a single fuel rod, using the LS-DYNA explicit finite element code. The key output of the modeling is fuel cladding strain, which is used in stress analysis and fatigue analysis to demonstrate fuel cladding integrity. This work also considers stress concentrations in the cladding due to the interaction of discrete fuel pellets with the cladding tube in bending load cases. This paper describes model development, defines the broader analytical methodology, and provides a validation of the models and the methodology through comparison to the test data collected during the MMTT. The validated models and analysis methodologies described in this paper are being applied in ongoing modeling and analysis work to evaluate other UNF transportation configurations that differ from the MMTT configuration.

INTRODUCTION
In 2017, the United States Department of Energy collaborated with Spanish and Korean organizations to perform a multimodal transportation test (MMTT) to measure shock and vibration loads imparted to used nuclear fuel (UNF) assemblies. This test used real fuel assembly components containing surrogate fuel mass to approximate the response characteristics of irradiated used nuclear fuel [1, 2]. Pacific Northwest National Laboratory (PNNL) was part of the test team and performed modeling and analysis using the test data to validate numerical models and analysis methods to predict the dynamic response of the cask and conveyance system,

including the structural-dynamic response of fuel assemblies and fuel cladding [3]. This work was done as a part of the DOE Spent Fuel and Waste Science and Technology (SFWST) program. The mission of the SFWST to program is to conduct research and development activities related to storage, transportation, and disposal of UNF. Within SFWST, the storage and transportation task examines issues associated with the extended storage and subsequent transportation of UNF. One gap in knowledge identified as high priority by SFWST concerned studying the shock and vibration loading environment that UNF is exposed to during transportation, and determining if this environment challenges cladding integrity [4]. The analytical work to date suggests that cladding integrity is not significantly challenged during normal conditions of transportation, but the authors are still finishing analyses to relate the MMTT test configuration to purpose-built UNF transportation systems. This paper discusses some of the models and analyses that have been completed for this task.

RAIL SHOCK AND VIBRATION LOADING ENVIRONMENT

The MMTT rail test collected shock and vibration data over three different rail transportation environments. The westbound (Baltimore, MD to Pueblo, CO) rail leg was performed via dedicated rail service, which provides a direct, nearly non-stop shipping service. In the westbound rail segment, just one interchange was required to transfer the railcar from one shipper to another. The captive track testing at TTCI (Transportation Technology Center, Inc.) was performed with a locomotive, instrumentation car, and in some specific tests an additional car for necessary added mass. The eastbound rail leg was performed using a general freight service, so the specific conditions are unknown. From the data, it is clear that the eastbound rail leg included many stops and interchanges, and it only reached St. Louis, MO before the data acquisition system exceeded its capabilities. The eastbound rail was affected by Hurricane Harvey, which disrupted train operations throughout the country in 2017.

The MMTT data shows a very benign shock and vibration loading environment for the fuel assembly. The primary basis for this assessment is the strain gage data, which recorded strains on the cladding that was less than 0.0001 in all three railroad environments. Accelerometer data was also collected on the fuel assemblies (and the other key components of the railcar system) but the relationship between acceleration and strain is not proportional in a dynamic loading environment. Physically, strain represents the deflection of a structure, while acceleration measures motion of a point on a body. Accelerometer measurements include some combination of rigid body motion and flexible body deflection.

When considering the data recorded in the MMTT for use in structural analysis, it is important to remember that instantaneous acceleration peaks are not equivalent to quasi-static loads. An illustration of this is the coupling test data recorded at TTCI, for a nominal 8 mph coupling event. The peak vertical acceleration recorded on the railcar deck was 7.24 g (1g = 9.81 m/s^2), a few inches higher on the cradle structure the acceleration was recorded as 6.42 g, and a few meters higher on the top of the cask it was recorded as 1.27 g. While the peak acceleration at all of these locations was over 1 g, the peak strain recorded on the cladding was less than 0.0001. The railcar deck and cradle accelerometer data imply mechanical shock loads on the system that could potentially cause much larger strains in the fuel cladding than actually occurred.

The motion of the cask, not the motion of the railcar or cradle, is believed to be the best basis for deriving loads on the fuel rods. Casks (or packages) are very heavy, with relatively thick steel walls, and compared to the railcar deck or the cradle are approximately rigid structures. Figure 1(A) shows the maximum power spectral density (PSD) of the two vertical cask accelerometer

signals in three different cases. ORE1 refers to Rail Event #1, the instance of maximum cask vertical acceleration recorded in the westbound rail, which was traced to a specific road crossing near Mckeen, Illinois. PB50 refers to the 50 mph pitch and bounce test performed at TTCI. SB50 refers to the 50 mph single bump test performed at TTCI. Both the PB50 and SB50 are standard railcar tests that are performed to demonstrate a railcar's compliance with Association of American Railroads (AAR) S-2043 [5] Figure 1(A) shows that the PSD's are all very similar, and that for analysis purposes, the TTCI tests provide a good basis for what the railcar can experience on the open rail.

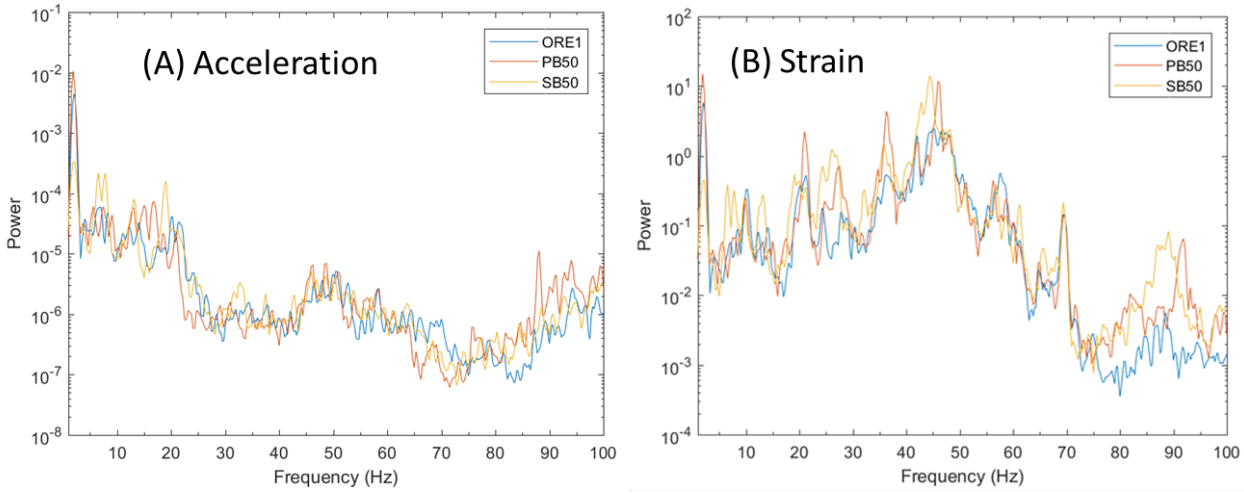

Figure 1. PSD's of acceleration and of strain during bounce events

Similarly, Figure 1(B) shows the maximum PSD of all strain gage channels in the same three cases. While ORE1, PB50, and SB50 are again very similar to each other, note that the frequency content of the strain gage data is very different from the frequency content of the cask accelerometer data. This is an indication that the fuel rods are responding and vibrating in a different frequency band (Figure 1(B)) than the base excitation (Figure 1(A)). The one frequency where both PSDs show a strong common component is around 2 Hz, which corresponds to the railcar suspension system. The first transverse bending mode of a fuel assembly is also around 2 Hz, but there is not enough room in a fuel basket for a fuel assembly to achieve significant transverse deflection. Figure 1(B) shows that higher frequencies, above 2 Hz and at least up to 100 Hz, are significant. These higher frequency components are expected to correspond to the spacer grid span natural frequencies, and represent the local response to excitation. Figure 1(B) presents a maximum PSD curve that encompasses all strain gages in the test, so data from different span lengths contribute to Figure 1(B).

One of the groundbreaking aspects of the MMTT is that it collected continuous shock and vibration data over long periods of time, for a representative UNF shipment. The trend in the data is that significant data is associated with track features, such as road crossings, but between track features there are large gaps of time that are filled with very low amplitude signal from the transducers. This fact is important for fatigue evaluations, where the loading over long periods of time is needed. The authors studied the Root-Mean-Square (RMS) of the data signals using a sliding 1 second and 10-second window in order to characterize how much of the time the system experienced significant loading compared to background noise threshold. The authors are still working on translating this MMTT test data into a cladding fatigue analysis methodology, but this topic is discussed in more detail in a later section of this paper.

Cask and Cradle and Railcar Modeling

Railcar dynamics modeling is a standard practice in the railroad industry to qualify railcars for interchange service by AAR. It is safe to assume that any railcar qualified to transport SNF is the USA will have railcar dynamics models built to demonstrate it meets AAR S-2043 [5] requirements, and it is also to be expected that a prototype railcar will tested at TTCI or an equivalent testing facility. Modeling and analysis related to the MMTT has demonstrated that railcar dynamics models are adequate for calculating transportation cask motion to use as loading conditions for structural dynamic analyses of fuel assemblies and fuel rods [3].

The key feature a railcar dynamics model needs is a representation of the transportation cask and its cradle (support structure). A single degree of freedom (SDOF) spring-mass-damper was sufficient to achieve agreement with test data from the MMTT. The calculated cask motion agreed reasonably well with the cask accelerometer data and using the calculated cask motion as base excitation to a single fuel rod structural dynamic model achieved reasonable agreement with strain gage data. The SDOF model requires a package mass (known), a spring stiffness (calculated from a modal analysis), and a damping value (which may need to be based on test data or assumptions). The MMTT data suggests that the range of damping for a realistic system could be in the range of 20% to 50% of critical damping. The MMTT was estimated to be close to 50% of critical damping between the cask and the railcar deck, although in that case a contributing factor was the presence of rubber mats between the bottom of the cradle and the top of the railcar deck.

Separate shaker table testing was performed [6] to test the damping characteristics of the rubber mat material used in the test, as well as plywood and steel. The shaker tests suggest that the component of total system damping contributed from rubber, plywood, and steel intermediate material could be 20%, 5%, and 5%, respectively. The conclusion from this study is that the rubber

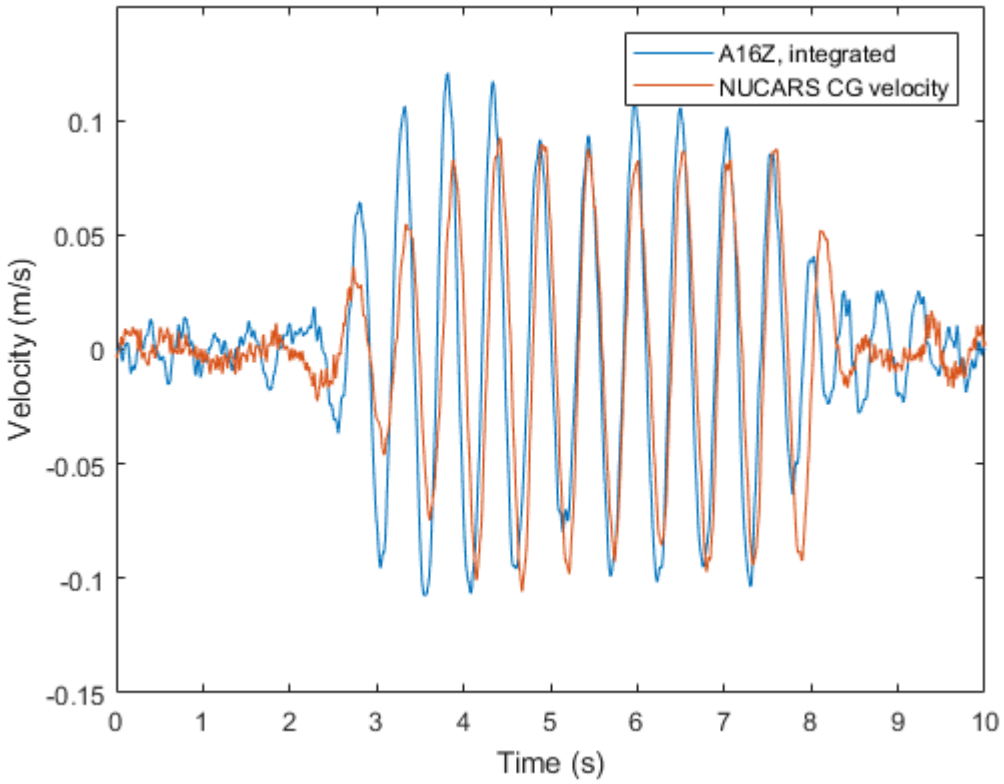

Figure 2. Modeled and measured cask velocities

mats used in the MMTT test contributed to a higher damping configuration than if plywood were used, or steel-on-steel contact was allowed. For analysis purposes, the authors recommend assuming 20% damping in the cask and cradle SDOF system as a conservative minimum damping value unless specific test data or analysis can support higher damping.

The end result of the railcar model is to generate the cask motion history that results from a set of velocity and track conditions. Cask motion is applied as a base excitation load to calculate fuel cladding stress and strain over time. A comparison of model calculated cask velocity to integrated accelerometer data is provided in Figure 2.

FUEL CLADDING STRUCTURAL DYNAMIC ANALYSIS

The LS-DYNA explicit finite element program was used to create structural dynamic finite element models to calculate fuel cladding response to dynamic loads. The MMTT collected cladding strain data over time, and that is the primary data used to benchmark and validate the cladding finite element models.

PNNL used a number of different finite element representations to study the MMTT results, including a full fuel assembly model, a column of fuel rods, or a single rod model. The most practical model for this task is a single rod model, because the fuel rod deflections are so small that rod-to-rod contact is not expected. The single rod model is shown in Figure 3. The key features of the model are that fuel and cladding is homogenized as an equivalent elastic beam with a constant cross section, and translational and rotational springs are used to represent the interaction of the fuel rod with the grid spacers. The spring constants were selected to match the MMTT test data, but they also could have been determined from proprietary fuel assembly design data.

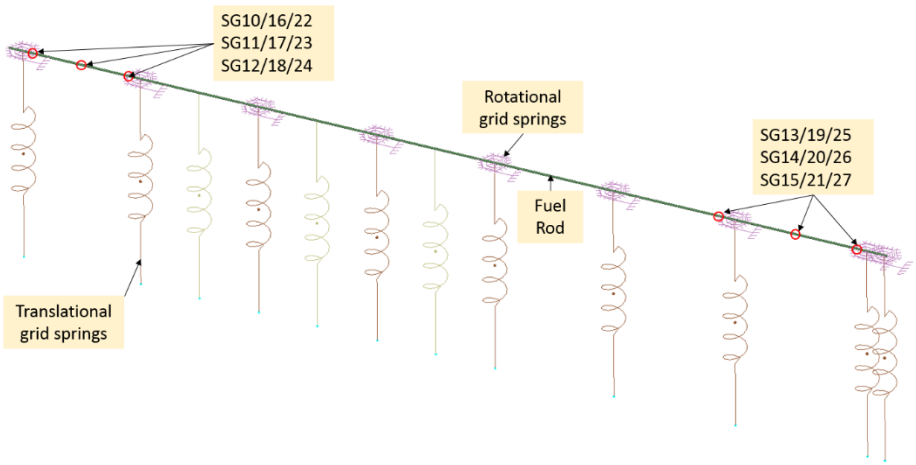

Figure 3. Single rod model representation

The single rod model was used to calculate the response of the fuel rod to loads from the MMTT. Table 1 lists the peak strains recorded at strain gage locations, as well as strains calculated from the single rod model based on excitation recorded in the MMTT (A15Z and A16Z). The last column lists the strains that are calculated when the single rod model uses the cask motion calculated in NUCARS [7] and plotted in Figure 2. The single rod model predictions show very good agreement with the data, especially when using the MMTT accelerometer data as input.

Reasonably good agreement is achieved when using the cask motion calculated from NUCARS, with a tendency to overestimate the strains. Nevertheless, both the test data and single rod model demonstrate that the strain encountered by the fuel rod is very small.

Table 1. Peak strains for unirradiated fuel rod, measured and predicted

Peak strain (uE) at SG locations				
		Single Rod Model		
Strain Gage	MMTT data	A16Z	A15Z	NUCARS Cask CG
SG10/16/22	4.7	6.4	7.5	7.5
SG11/17/23	10.4	10.3	9.9	10.8
SG12/18/24	7.3	8.5	8.0	8.1
SG13/19/25	9.6	11.3	9.7	10.6
SG14/20/26	10.0	11.4	10.4	14.9
SG15/21/27	8.9	10.2	9.9	13.7

The single rod model was also used to calculate the response of fuel rods in the irradiated condition. The homogenized fuel rod stiffness (EI) was increased to represent a state where the fuel is fully bonded to the cladding. The typical EI used in the fuel rod models to represent the MMTT is 14 N-m^2, which represents the room temperature cladding tube alone and neglects any stiffness contribution from the surrogate mass inside the tube. Fully bonded fuel in the irradiated condition is estimated to be in the range of 30 N-m^2 to 55 N-m^2 [8]. A value of 40 N-m^2 was chosen to estimate the irradiated condition. Table 2 lists the MMTT test condition and irradiated condition response. Overall, smaller strains were predicted for the irradiated fuel rod. However, the magnitude of this change was not the same for all input time histories used. Using the accelerometer data from the MMTT, the resulting strains were several times smaller than their unirradiated counterparts. On the other hand, when using the accelerations output by NUCARS, the strains were only slightly smaller. This is because while the higher rigidity in the irradiated state tends to reduce strains, it also shifts the natural frequency of the fuel rod. Compared to the test data, the NUCARS model tended to predict cask accelerations with a stronger response in the 65-80 Hz range, which overlaps with the resonance frequencies of the fuel rods in the irradiated state. Evidence of natural frequency effects can be seen when comparing the last columns of Table 1 and Table 2. Note that the location of maximum strain changes between the two cases, even when the excitation load history remains the same. While the choice of 40 N-m^2 for irradiated fuel is demonstrated to produce lower strains in this load case, the authors intend to complete a sensitivity study over the range of 30 N-m^2 to 55 N-m^2 to quantify the effect of fuel rod stiffness on the calculation of peak strain.

Note that the preceding analyses assume the fuel rod is a homogenous elastic beam and nominal stresses on the exterior of the cladding surface are reported. In a real fuel rod, the stress state of the cladding is expected to be affected by the fuel pellets inside the cladding. Experimentally, Oak Ridge National Laboratory (ORNL) cyclic integrated reversible-bending fatigue tester (CIRFT) test experience observed that cladding failures usually occur at the pellet-pellet interface [9]. This was anticipated for two reasons: 1) At the pellet-pellet interface no pellet material is present to bond with the cladding inner diameter because of the pellet chamfers, because of this, the rod no longer acts as a composite structure locally yielding a reduced EI at this location. 2) Pellet chamfer design is highly optimized, however the chamfer itself still acts as a source for

stress concentration. In addition to the effects associated with the pellet chamfers, additional sources of stress concentration can occur on a rod. These include stress concentration due to fretting wear, damaged pellets, interaction with the assembly hardware, etc. The authors are currently performing analyses to study stress concentrations in cladding, to determine how best to account for the anticipated stress concentration. Note that with the low magnitude of strains, the stress concentration is not expected to be significant for NCT transportation shock and vibration loading, but it could be more important in NCT package drops or hypothetical accident conditions.

Table 2. Peak strains for irradiated fuel rod, predicted

Peak strain (uE) at SG locations (Irradiated Rod - 40 N-m^2)			
	Single Rod Model		
Strain Gage	**A16Z**	**A15Z**	**NUCARS Cask CG**
SG10/16/22	1.6	1.6	6.1
SG11/17/23	3.0	3.1	11.7
SG12/18/24	2.2	2.2	8.0
SG13/19/25	3.8	2.6	12.0
SG14/20/26	3.9	2.7	7.3
SG15/21/27	3.5	2.4	6.0

FUEL CLADDING STRAIN ENERGY

One useful feature of the explicit finite element formulation is that strain energy is calculated for deformable bodies throughout the transient solution time. The fuel rod strain energy calculated by LS-DYNA for dynamic load cases from the MMTT was only on the order of 1 mJ, which is roughly equivalent to the kinetic energy in a relatively large raindrop or the kinetic energy of a flying wasp. These physics examples are an effective way of communicating the relatively low shock and vibration energy experience by the cladding during normal conditions of transport.

To check LS-DYNA's strain energy calculation, the relationship between strain and strain energy in a full cladding tube was explored. Equation (1) describes the relationship between strain and strain energy in an axial tension loading condition. In Equation (1), U is strain energy, V is volume, and E is modulus of elasticity. For a 4m long fuel rod cladding, this calculation represents the total strain energy in the cladding, with strain evenly distributed along its length, as if it was in quasi-static tension loading. Figure 4 shows the relationship between strain energy and microstrain in the cladding. This paper uses the symbol uE to represent microstrain (1 uE = 0.000001 m/m). From the figure, note that 1 mJ of strain energy relates to an average axial strain of about 20 uE, which is a typical peak strain value recorded during the MMTT. The maximum strain recorded in the MMTT was about 100 uE, which relates to 28 mJ, if the cladding was in a uniform state of tension. The finite element model calculated a total strain energy of about 5 mJ for that maximum load case, but that takes into account local rod bending and the transient vibration response over time. Figure 4 supports the conclusion that the strain energy calculated by the LS-DYNA model is in the right order of magnitude, and is extremely small. The raindrop and flying insect analogies remain appropriate.

$$U = \frac{1}{2} VE \bullet (strain)^2 \quad (1)$$

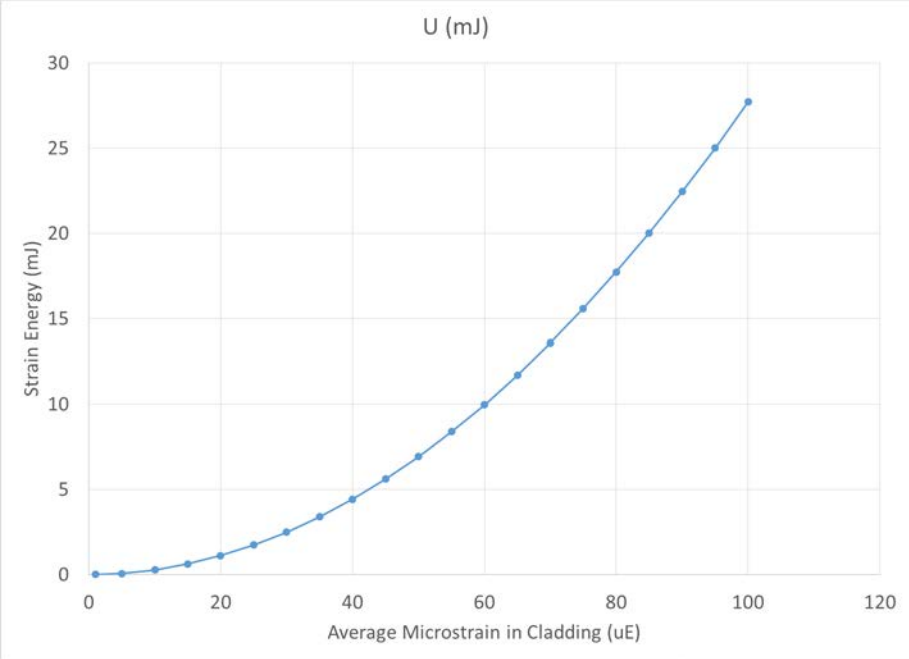

Figure 4. Strain energy as a function of cladding strain

FUEL CLADDING FATIGUE ANALYSIS

A full cladding fatigue analysis was performed for the MMTT westbound rail data set, which was approximately 2000 miles of rail transportation over a period of about 6 days. ASTM rainflow counting was applied to the strain gage signals to calculate the amplitude and number of strain cycles. Miner's rule was used to calculate accumulated damage from the cycles based on the O'Donnell S-N curve. The details of this fatigue calculation are reported in [3]. The final conclusion was that accumulated fatigue damage was approximately zero. Another way to look at the analysis is that it would take over 10 billion 2,000 mile train transportation trips before a cladding fatigue failure would be expected.

One important parameter of any fatigue analysis is the number of strain cycles. It is typical to perform a structural analysis on fuel cladding by choosing a loading scenario and assuming that scenario repeats a certain number of times. In a hypothetical 2,000 mile transportation, the estimated number of cycles could be very high. For example, a train moving at 50 mph would take 40 hours to reach its destination. If there is a 60 Hz vibration in the fuel cladding, that vibration could be expected to repeat almost 9 million times (or 9E+6 strain cycles). However, the westbound rail leg of the MMTT took closer to 59 hours (of train movement), which would increase the strain cycle estimate to 1.3E+7 cycles. The MMTT data suggests that 60 Hz is a relatively important vibration frequency, but the total number of cladding strain cycles that were greater than 10 uE was only about 4E+3, or orders of magnitude lower than might be expected.

The observation from the MMTT test data is that significant shock and vibration only happens rarely during transportation, such as when the train crosses a road, or some other significant track feature. When the train is in a steady-state condition, the vibrations and the signal strength from the strain gages drops to a very low threshold. As long as the steady state vibration

remains negligible, a fatigue analysis only needs to consider the number of road crossings and other sources of perturbation along a given route. These can be calculated or estimated based on maps or general information about the rail system.

The authors are still finalizing methods for generating long duration fatigue analyses based on the MMTT data. An illustration of the data and the variation in shock and vibration signal strength is provided in Table 3. Strain gage SG8-0 on the westbound rail leg of the MMTT is used because it had the highest average RMS signal strength. The reported RMS values are based on a 1 second sliding RMS window. The westbound rail test had a total duration of 144 hours, but for 85 hours the railcar was at rest, and for 59 hours the railcar was in motion. The strongest 1 hour of signal (i.e., the maximum 3,600 discrete 1-second RMS values) is separated from the 59 hours of railcar movement to define two categories, Steady State Motion and Strong Vibration, each with distinct RMS signal ranges. The Strong Vibration category might include all significant shock events (e.g., road crossings) witnessed in the westbound MMTT, but this has not been confirmed. Still, binning and categorizing the strain gage signals in this way provides insight into the long duration shock and vibration environment. The highest RMS value is 9.7 uE, but if this peak signal strength was used to define 59 hours of hypothetical fatigue loading it would be much stronger than the actual 59 hour RMS average, which on a time-weighted basis is closer to 1.55 uE. While a highly conservative fatigue analysis can be adequate for demonstrating safety, the authors are working to develop a more realistic methodology for defining fatigue loads for fuel cladding.

Table 3. RMS ranges of strain gauge SG8-0 data for dedicated rail

	Strain Gage RMS Range	Average RMS	Time (hrs)	Trip percentage (%)
Rest	0-0.3 uE	0.06 uE	85 hrs	59%
Steady State Motion	0.3-3.7 uE	1.5 uE	58 hrs	40%
Strong Vibration	3.7-9.7 uE	4.3 uE	1 hr	1%

ONGOING WORK

The authors are applying the models and analytical methods discussed in this paper (and presented in more detail in [3]) to an analysis of the Atlas railcar. This work should be completed in 2019 and documented in a DOE report that should be released to the public in late 2019.

CONCLUSIONS

The shock and vibration environment witnessed in the MMTT is very mild, and railcar dynamic models reasonably agree with test data. . While peak accelerations were recorded in multiples of gravity, the stain recorded in the cladding is a better indication of the structural loads transmitted to the fuel cladding.

The single fuel rod model used in this work agrees well with MMTT test data. Substituting irradiated UNF material properties into the single rod model results in lower peaks strains relative to the non-irradiated condition. While this is true for the test case, a sensitivity study is recommended to quantify the sensitivity to fuel rod natural frequency within the expected range of stiffness for irradiated UNF. It is recognized that changes in fuel rod stiffness (and natural frequency) can alter the fuel rod's response to dynamic excitation.

The fuel cladding strain energy calculated in LS-DYNA agrees with expectations, based on the energy implied by strain gage data.

The authors are working to develop a fatigue analysis methodology that matches observations from the MMTT. The average shock and vibration RMS signal strength over 59 hours of rail transportation (1.55 uE) is much lower than the peak second (9.7 uE), or the peak average hour (4.3 uE).

ACKNOWLEDGEMENTS

The authors would like to express our sincere thanks to the project's DOE sponsors, Ned Larson and John Orchard for supporting and funding this work. We would also like to thank our collaborators on the multimodal transportation test campaign (MMTT), including staff from Sandia National Laboratories, ENSA, KAERI, and TTCI., We would also like to acknowledge and express our appreciation for additional organizations that helped make the MMTT possible with their contributions, including: ENUSA, ENRESA, KORAD, KEPCO NF, ANL, and Coordinadora.

REFERENCES

1. McConnell PE, SB Ross, CA Grey, WL Uncapher, M Arviso, R Garmendia, IF Perez, A Palacio, G Calleja, D Garrido, AR Casas, LG Garcia, W Chilton, DJ Ammerman, J Walz, S Gershon, SJ Saltzstein, K Sorenson, NA Klymyshyn, BD Hanson, R Pena, and R Walker. 2018. Rail-Cask Tests: Normal-Conditions-of- Transport Tests of Surrogate PWR Fuel Assemblies in an ENSA ENUN 32P Cask. SFWD-SFWST-2017-000004, Sandia National Laboratories, Albuquerque, New Mexico.
2. Kalinina, EA, C Wright, N Gordon, SJ Saltzstein, L Lujan, KM Norman. 2018. Data Analysis of ENSA/DOE Rail Tests. 2018. SFWD-SFWST-2018-000494, Sandia National Laboratories, Albuquerque, New Mexico.
3. Klymyshyn N.A., P. Ivanusa, K. Kadooka, C.J. Spitz, P.J. Jensen, S.B. Ross, and B.D. Hanson, et al. 2018. Modeling and Analysis of the ENSA/DOE Multimodal Transportation Campaign. 2018. PNNL-28088. Richland, WA: Pacific Northwest National Laboratory.
4. Hanson B., Alsaed, H., Stockman, C., Enos, D., Meyer, R., and Sorenson, K. *Gap Analysis to Support Extended Storage of Used Nuclear Fuel*. FCRD-USED-2011-000136 Rev. 0, PNNL-20509, (2012).
5. AAR (Association of American Railroad). 2017. "Performance Specification for Trains Used to Carry High-Level Radioactive Material." AAR S-2043, Wood Dale, Illinois.
6. Kalinina EA, C. Wright, D.J. Ammerman, C.A. Grey, and M. Arviso. Shaker Table Test. 2019. Sandia National Laboratories. M3SF-19SN010202021. SAND2019-3120R.
7. TTCI (Transportation Technology Center, Inc.). January 2018. NUCARS User Manual, Version 2018.1. Pueblo, Colorado.
8. Klymyshyn N.A., P.J. Jensen, and N.P. Barrett. 2016. "Modeling Used Fuel Response to 30 cm Package Drops." Proceedings of the 18th International Symposium on the Packaging and Transportation of Radioactive Materials, PATRAM 2016. September 18-23, 2016, Kobe, Japan.
9. Wang, J.-A., H. Wang, H. Jiang, Y. Yan, B. B. Bevard, J. M. Scaglione. 2016. "FY 2016 Status Report: Documentation of All CIRFT Data including Hydride Reorientation Tests." Oak Ridge National Laboratory, ORNL/SR-2016/424, September 14, 2016.